Remote Sensing of Environment 113 (2009) 1101–1111

Contents lists available at ScienceDirect

Remote Sensing of Environment

journal homepage: www.elsevier.com/locate/rse

Tracking seasonal drought effects on ecosystem light use efficiency with satellite-based PRI in a Mediterranean forest

A. Goerner [a,*], M. Reichstein [a], S. Rambal [b]

[a] Max Planck Institute for Biogeochemistry, 07745 Jena, Germany
[b] CEFE-CNRS, 34293 Montpellier cedex 5, France

ARTICLE INFO

Article history:
Received 17 July 2008
Received in revised form 3 February 2009
Accepted 3 February 2009

Keywords:
Photochemical reflectance index
Light use efficiency
Gross primary productivity
Mediterranean

ABSTRACT

Gross primary productivity (GPP) changes occur at different time-scales and due to various mechanisms such as variations in leaf area, chlorophyll content, rubisco activity, and stomatal conductance. Diagnostic estimates of primary productivity are obviously error prone when these changes are not accounted for. Additional complications arise when factors inuencing a biome-specific maximum light use efficiency (LUE) must be estimated over a large area. In these cases a direct estimation of ecosystem LUE could reduce uncertainty of GPP estimates. Here, we analyse whether a MODIS-based photochemical reectance index (PRI) is a useful proxy for the light use efficiency of a Mediterranean *Quercus ilex* forest. As the originally proposed reference band for PRI is not available on MODIS, we tested the reference bands 1 (620–670 nm), 4 (545–565 nm), 12 (546–556 nm), 13 (662–672 nm), and 14 (673–683 nm) using different atmospheric correction algorithms. We repeated the analysis with different temporal resolutions of LUE (half-hourly to daily). The strongest correlation between LUE and PRI was found when considering only a narrow range of viewing angles at a time (especially 0–10° and 30–40°). We found that the MODIS-based PRI was able to track ecosystem LUE even during severe summer time water limitation. For this Mediterranean-type ecosystem we could show that a GPP estimation based on PRI is a huge improvement compared to the MODIS GPP algorithm. In this study, MODIS spectral band 1 turned out to be the most suitable reference band for PRI, followed by the narrow red bands 13 and 14. As to date no universally applicable reference band was identified in MODIS-based PRI studies, we advocate thorough testing for the optimal band combination in future studies.

© 2009 Elsevier Inc. All rights reserved.

1. Introduction

Many diagnostic models of terrestrial ecosystem productivity compute gross primary productivity (GPP) as the product of the amount of absorbed photosynthetically active radiation (aPAR) and a light use efficiency term (Kumar & Monteith, 1981; Monteith, 1972, 1977). aPAR can be conceived as the product of photosynthetically active radiation incident on the ground (incPAR) and the fraction of incPAR absorbed by the vegetation (faPAR). These entities can be derived from global meteorological fields and satellite products, respectively (e.g. Goetz et al., 1999; Ruimy et al., 1994).

It follows from the above that light use efficiency (LUE) is the ratio of productivity to aPAR. In this study, we refer more specifically to LUE as mols of CO_2 captured per mol of photons absorbed. LUE is inherently variable as it is determined by the quantum efficiency of photosynthesis (Grace et al., 2007). Photoprotective mechanisms reduce the photosynthetic quantum efficiency at times of environmental stress (such as temperature extremes, water or nutrient deficit, exposure to high light intensities, e.g. Green et al., 2003; Runyon et al., 1994). In addition, decreased stomatal conductance in times of drought will reduce available CO_2 and thus the rate of photosynthesis (Galmés et al., 2007).

In current diagnostic models, the light use efficiency (LUE) term is implemented either as a constant (sometimes stratified according to plant functional type) or as a (biome-specific) maximum LUE that is reduced by scalars representing environmental stress (Yuan et al., 2007). It has been shown that this look-up table approach is not able to capture the full range of productivity dynamics, especially at finer temporal scales (Schwalm et al., 2006; Turner et al., 2002, 2006), primarily due to inaccurate maximum LUE estimates (Martel et al., 2005). Additional uncertainty arises when environmental drivers reducing maximum LUE need to be estimated on a global scale (Heinsch et al., 2006). Also, current remote-sensing based models have difficulties to detect drought stress (Turner et al., 2005) unless soil water content is accounted for (Leuning et al., 2005), which is difficult on a global scale. If we can obtain direct estimations of LUE from remote sensing data, this will lead us to more accurate calculations of GPP. We would need an integrative indicator of how photosynthetic capacity is controlled by environmental stress. Traditional vegetation indices such as the normalised difference vegetation

* Corresponding author.
E-mail address: anna.goerner@bgc-jena.mpg.de (A. Goerner).
URL: http://www.bgc-jena.mpg.de/bgc-mdi/ (A. Goerner).

0034-4257/$ – see front matter © 2009 Elsevier Inc. All rights reserved.
doi:10.1016/j.rse.2009.02.001

index (NDVI) seem inappropriate for this task because they mainly measure greenness and can only track decreases in photosynthetic activity when they lead to yellowing or shedding of leaves (Gamon et al., 1995).

Another option to estimate LUE employs the mechanisms with which plants protect their chloroplasts from the creation of harmful reactive oxygen species. This danger arises if plants are subject to more light than they can use for photosynthesis. The photoprotection process includes changes in the trans-thylakoid pH-gradient, conformational changes in the chloroplasts, and the de-epoxidation of violaxanthin via antheraxanthin to zeaxanthin (Demmig-Adams & Adams, 2006). The formation of zeaxanthin is necessary to dissipate excess light as heat (Demmig et al., 1987) and at the same time decreases reflectance in a narrow wavelength range centred around 531 nm (Gamon et al., 1990).

The photochemical reflectance index (PRI) combines reflectance at this wavelength (ρ_{531}) with a reference wavelength insensitive to short-term changes in light energy conversion efficiency (usually 570 nm, ρ_{570}) and normalises it (Gamon et al., 1992; Penuelas et al., 1995):

$$\mathrm{PRI} = (\rho_{531} - \rho_{570}) / (\rho_{531} + \rho_{570}) \quad (1)$$

Many studies have been conducted at the leaf and canopy scale with plants representing different photosynthetic pathways and ecosystems. In these studies PRI was well correlated with the epoxidation state of xanthophylls and LUE (Penuelas et al., 1995; Sims & Gamon, 2002; Stylinski et al., 2002; Weng et al., 2006). A strong relationship between PRI and LUE could also be shown for plants suffering from environmental stress affecting energy dissipation pathways, namely nitrogen limitation (Gamon et al., 1992), high ozone concentrations (Meroni et al., 2008), water limitation (Suarez et al., 2008), or flooding (Naumann et al., 2008). Several studies tested the performance of PRI as an indicator of LUE at ecosystem scale. The test was successful for boreal ecosystems, although in these studies LUE was based on incident PAR rather then aPAR (Nichol et al., 2000; Nichol et al., 2002). In predominantly water limited ecosystems the applicability of PRI as LUE proxy might be limited to vegetation types that are not subject to strong changes in canopy structure (Filella et al., 2004; Sims et al., 2006).

Only few studies have attempted an investigation of the PRI–LUE relationship with satellite data so far. Limiting factors are probably the number of space-borne sensors with the necessary narrow spectral bands and the pre-processing required for PRI calculation (correction for atmospheric disturbances and BRDF effects). Up to now, some studies on boreal, temperate, and Mediterranean type ecosystems have successfully tested MODIS-derived PRI as a proxy for ecosystem LUE (Drolet et al., 2005; Drolet et al., 2008; Garbulsky et al., 2008; Rahman, 2004). MODIS seems to be the most appropriate sensor currently available to test space-borne PRI because one of its 10 nm wide "ocean bands" is centred at 531 nm. The not too narrow spectral bands might actually be an advantage, given that Gamon et al. (1992, 1993) found that the optimum wavelength for LUE tracking varies in between species and canopy types. The temporal resolution of MODIS data is comparatively high. Since both the Terra and the Aqua satellites have a roughly identical MODIS sensor aboard, two or more data acquisitions can take place under cloud free conditions. The MODIS observation footprint for the required bands is about 1 km^2 if the sensor view zenith angle is limited to no more than 40° (Wolfe et al., 1998). This is in the same order of magnitude as the footprint of eddy covariance towers, although the fetch of eddy covariance systems depends on measurement height, the surface roughness, and the characteristics of the boundary layer as well as the atmospheric stability (Rebmann et al., 2005). We can assume comparable conditions in the remotely sensed area and the flux tower source area when restricting the analysis to towers located in a large enough homogeneous area. Hence, for some carefully selected eddy covariance sites a comparison to ground based estimates of light use efficiency is possible. At a homogeneous site the results will not be compromised if some of the 1 km MODIS pixel are not properly centred on the eddy covariance tower and do only partially coincide with the flux-tower footprint area.

Table 1
Bandwidth of the MODIS' spectral bands used in this study.

Band	Bandwidth (nm)	Use in this study
1	620–670	PRI, NDVI, EVI
2	841–876	NDVI, EVI
3	459–479	EVI
4	545–565	PRI
11	526–536	PRI
12	546–556	PRI
13	662–672	PRI
14	673–683	PRI

The quality flags associated with every MODIS pixel allow for screening according to cloud cover and the general usefulness of the data. Given an ideally homogeneous study site the following issues need to be taken into account when interpreting PRI values in 1 km MODIS pixels. The sensor lacks a spectral band at 570 nm (c.f. Table 1), hence another reference band needs to be chosen. A modelling study by Barton and North (2001) indicates that differences in viewing and illumination geometry are likely to influence PRI. A stringent atmospheric correction should be performed in order to avoid variations simply due to differences in atmospheric composition (Grace et al., 2007). In addition to these difficulties, studies at a regional scale (or larger) would ultimately need to deal with sub-pixel heterogeneity.

Hardly any space-borne LUE estimation has been undertaken so far for more water limited ecosystems. Garbulsky et al. (2008) estimated LUE for an evergreen Mediterranean oak forest in Castelporziano, Italy. However, the trees there do have access to groundwater (Reichstein et al., 2002), thus water limitation is not severe. It is important to bridge this gap because the area affected by drought is about to increase: According to Christensen et al. (2007), it is likely that annual precipitation will decrease in several regions, among them Central Europe, the Mediterranean, the south-western US, Central America and Southern Australia. For the Mediterranean this goes along with an increased risk of summer drought (Giorgi, 2006). It is crucial to improve the performance of diagnostic models with respect to drought events. Upgraded data-oriented models can then serve as benchmarks to improve current process models.

Changes of LUE in drought-tolerant evergreen species are often not paralleled by changes in NDVI or canopy structure (Gamon et al., 1992; Running & Nemani, 1988). Thus sclerophyll dominated ecosystems seem to be a good starting point for testing the performance of satellite-based PRI as LUE proxy. In this study we therefore concentrate on a Mediterranean *Quercus ilex* forest. Special emphasis will be placed on the capability of MODIS-based PRI to estimate LUE during drought events because this is where current diagnostic models of GPP have deficiencies. Specifically, we will assess which reference band is most suitable for this application and test the influence of different methods of atmospheric correction on the PRI–LUE relationship. Though, for reasons detailed above, we do not expect a relationship between LUE and NDVI or Enhanced Vegetation Index (EVI) for this ecosystem, we include these indices in this analysis as benchmarks.

2. Methods

2.1. Study site and data

For this study, we focused on a flux tower site in the Puéchabon state forest (43.7414° N, 3.5958° E) in southern France, 35 km north-

west of Montpellier. The *Quercus ilex* forest has been managed as a coppice for centuries, the last cut occurred in 1942. Allard et al. (2008) give a detailed site description, but we cite the most relevant characteristics here. The average tree height is about 5 m, the overstorey leaf area index (LAI) stated as 2.8 ± 0.4). The main species in the shrubby, sparse understorey (<2 m) are *Buxus sempervirens*, *Phyllirea latifolia*, *Pistacia terebinthus*, and *Juniperus oxycedrus*. The climate is of Mediterranean type, with an annual precipitation of ca. 900 mm (ranging from 550–1550 mm for 1984–2006) of which 80% occur between September and April. A reason to chose the Puéchabon site for this analysis is the role of *Quercus ilex* as one of the dominant species in Mediterranean type ecosystems (Terradas, 1999), covering about 6.55×10^4 km^2 (Quézel & Médail, 2003). Our analysis of the entropy, a quantity describing data homogeneity (Clausi, 2002), of a Landsat scene subset including the flux tower indicates that the site is homogeneous at the MODIS spatial resolution (Fig. 1, similar entropy levels in ca. 1 km distance from flux tower). The variations in surface properties observable within ca. 1 km around the flux tower are characteristic for the whole area covered by *Quercus ilex* growing on hard karstic limestones (ca. 4000 km^2) (Lacaze et al., 1994). Moreover, the flux tower footprint reliably represents the targeted land cover type (Goeckede et al., 2008). Comparability of remote sensing data and in-situ measurements is therefore granted.

In this study we look at the years 2002–2005 because satellite data as well as flux and meteorology data were available for this time span. Processing of the flux data has been performed according to the standard CarboEurope methods (Papale et al., 2006; Reichstein et al., 2005). Together with micro-meteorological data they were extracted from the LaThuile database (http://www.fluxdata.org/DataInfo/Dataset 20Doc 20Lib 20DR1/DataSetInfoDR1.aspx). The half-hourly GPP values were quality-checked with the flags included in the LaThuile data set. As a result of the standardised partitioning of the net CO_2 flux (GPP = − net ecosystem exchange + ecosystem respiration) GPP observations can become negative. When the true value is close to zero, the statistical random error might induce negative GPP values. Only 0.46% of the night time GPP values (with photosynthetic photon flux density <100 μmol m^2 s^{-1}) are lower than zero and were excluded from the analysis. Furthermore we used half-hourly incident photosynthetically active radiation (included in LaThuile data set) and below canopy photosynthetically active radiation data (bcPAR, available from principal investigator, i.e. Serge Rambal). BcPAR is calculated as an average of 14 upward looking PAR sensors installed at different places below the canopy. Incident PAR was measured with an upward looking PAR sensor mounted on the eddy covariance tower. We filtered the PAR values for measurement errors (i.e. reject PAR <0 and standard deviation (bcPAR) >600 μmol m^{-2} s^{-1}). As faPAR values we used estimates derived from half-hourly incPAR and below canopy PAR as well as the operational MODIS faPAR data.

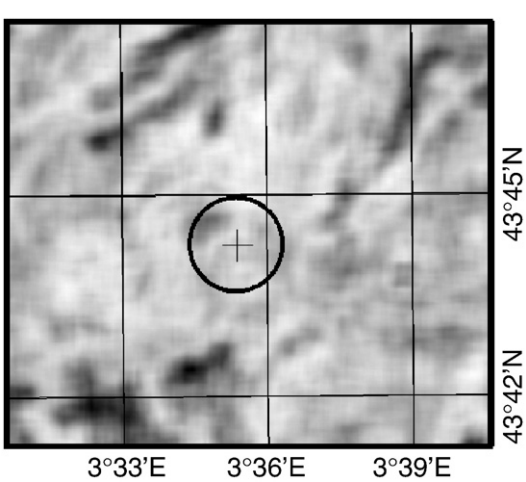

Fig. 1. Entropy calculated for the red band of a Landsat ETM+ scene (13. Aug. 2001). The location of the Puéchabon flux tower is indicated by a cross. The circle marks the relatively uniform area in which a MODIS pixel containing the tower will be positioned (radius 1 km + 300 m uncertainty). Light tone: high entropy, dark tone: low entropy.

We used soil moisture data to identify periods of water stress. The daily time course of soil water storage (mm) was simulated with a soil water balance model (Rambal, 1993) and further compared with monthly profiles of soil water content measured with a neutron probe and integrated over the rooting depth (c.a. 4.5 m). The relationships between simulated and observed values showed very close agreement ($r^2 = 0.87$).

2.2. Benchmark ecosystem light use efficiency

In this study, the light use efficiency (LUE) of an ecosystem is defined as the overall production of photosynthates per unit of absorbed photosynthetically active radiation. After Monteith (1972) this can be expressed as

$$\mathrm{GPP} = \mathrm{LUE} * \mathrm{faPAR} * \mathrm{incPAR} = \mathrm{LUE} * \mathrm{aPAR} \tag{2}$$

where GPP is gross primary productivity, PAR is incident photosynthetically active radiation, aPAR is the absorbed PAR, and faPAR is the fraction of PAR absorbed by the vegetation. LUE can either be seen as the ratio of GPP and aPAR or as the slope of a—possibly non-linear—function relating GPP to aPAR. To see whether differences arise from these two concepts, we used both as benchmarks to test the performance of several vegetation indices. The GPP values used in this context stem from the half-hourly eddy covariance data.

2.2.1. Light use efficiency solely based on site data

At the half-hourly scale, the fraction of absorbed photosynthetically active radiation (faPAR) was calculated as

$$\mathrm{faPAR} = 1 - \frac{\mathrm{bcPAR}}{\mathrm{incPAR}} \tag{3}$$

We decided to use the more common term faPAR for what strictly speaking is the fraction of intercepted PAR (fIPAR) (Gower et al., 1999). Nighttime values (with incPAR <100 μmol m^{-1} s^{-1} and outliers were screened out. Outliers were identified within a moving window as

$$X < Q_1 - \mathrm{IQR} \ \cup \ X > Q_3 + \mathrm{IQR} \tag{4}$$

where X are the data tested for outliers, Q_1 and Q_3 are the first and third quartiles, and IQR is the interquartile range. The standard deviation in below canopy PAR of the discarded observations was three times as high as in the full data set. The filtered half-hourly faPAR was then multiplied with the quality checked half-hourly incident PAR to obtain absorbed photosynthetically active radiation (aPAR). Light use efficiency was subsequently calculated as the ratio of half-hourly GPP and half-hourly aPAR. As the LUE in this study is calculated as $\frac{\mu\mathrm{mol\ CO_2}}{\mu\mathrm{mol\ photosynthetic\ photons}}$, it is essentially a dimensionless quantity. We also tested whether it is more meaningful to aggregate the half-hourly data and hence minimise noise. Thus we applied moving average filters to the half-hourly GPP, incPAR, and faPAR values, with window sizes of 90, 150, and 210 min. LUE was calculated both as ratio of averaged GPP and original half-hourly aPAR and as ratio of averaged GPP and aPAR derived from averaged incPAR and faPAR. Light use efficiencies were also calculated as a daily ratio. Daily averages of the original quality checked GPP, incPAR, and bcPAR data were used to calculate first a daily average faPAR and then aPAR and LUE.

To see whether we can obtain a better grip on the diurnal variations, we calculated LUE as the slope of half-hourly GPP and aPAR.

This variety of LUE was defined as the slope of a linear function fitted to the half-hourly GPP and aPAR values of each day. For 37% of the days the goodness of fit (r^2) was less than 0.6, thus fitting a linear function to the half-hourly GPP and aPAR values of these days is somehow arbitrary. As this occurred predominantly in low LUE conditions we did not reject those slopes in order to avoid biasing the data. In case of negative slopes on some summer days with low midday GPP observations the slope was set to 0.

2.2.2. Light use efficiency based on site data and MODIS faPAR

Collection 5 MODIS faPAR (Myneni et al., 2002) was downloaded separately for the Terra and Aqua platform as ASCII subsets from the Oak Ridge National Laboratory DAAC website (http://www.modis.ornl.gov/modis/index.cfm). In these data sets each faPAR value is representative of a period of eight consecutive days. To reduce gaps we merged the Terra and Aqua data sets. Preliminary tests with the individual MODIS faPAR time series revealed that the MODIS product is prone to underestimating faPAR for this site compared to bcPAR/incPAR based estimates, especially in winter time. Thus, whenever two MODIS faPAR estimates were available for the same period, we kept the higher one for the combined data set. We calculated another version of LUE through dividing average daily GPP values by the product of the MODIS faPAR values and average daily incPAR.

2.2.3. Light use efficiency as obtained from the MODIS biome property look-up table (BLUT)

To assess the performance of vegetation index-based LUE proxies we also calculated the LUE in the way it is operationally used in the MODIS GPP algorithm (Heinsch et al., 2003). In this approach, a biome-specific maximum light use efficiency is reduced by a vapour pressure deficit scalar and a minimum temperature scalar. These attenuation scalars are calculated from daily VPD and $T_{\min}$ based on linear ramp functions, the parameters of which are contained in the biome property look-up table (BPLUT). We used site measurements instead of the 1° by 1.25° NASA Data Assimilation Office (DAO) data routinely fed into the MODIS GPP algorithm to exclude mismatches between DAO and site meteorology as a source of error.

2.3. Remote sensing based estimates of light use efficiency

2.3.1. Acquisition and atmospheric correction of MODIS data

To process the MODIS data for this study we modified the procedure described by Drolet et al. (2005). Five MODIS products were downloaded from the Level 1 and Atmosphere Archive and Distribution System (http://ladsweb.nascom.nasa.gov) and the Earth Observing System data gateway (http://redhook.gsfc.nasa.gov/imswww/pub/imswelcome). Of those products, from both the Terra and Aqua satellite, we selected all scenes containing the tower location. The MOD/MYD021KM product comprises at-sensor calibrated radiances in 1 km spatial resolution. From that product we used the spectral bands listed in Table 1. The MOD/MYD03 product has the same spatial extent and resolution and provides the geographic coordinates as well as the solar and sensor zenith and azimuth angles of each pixel. These geolocation data were used to extract the spectral information of the pixel closest to the tower location. For the same location aerosol optical thickness was extracted from the MOD04 product and satellite-based estimates of cloud coverage were obtained from the MOD35 product. To account for the variation in reflectance introduced by the way of processing, we tested 4 different modes of atmospheric correction: With the 6S model (Vermote et al., 1997) atmospheric correction was performed assuming uniform Lambertian reflectance. Moreover, a dark object subtraction (DOS) approach has been taken to correct the spectral data. We also included at-sensor-reflectances in the comparison, i.e. without any correction for atmospheric disturbance and geometric effects.

Prior to the atmospheric correction with 6S those acquisition dates were discarded where the quality flags attached to the MODIS products indicated cloud cover, saturation of a detector, or poor estimates of atmospheric optical thickness. In addition, only scenes with a sensor viewing angle at the tower site of no more than 40° were retained to ensure equal spatial resolution (Wolfe et al., 1998). From preliminary experiments we know that the effect of BRDF correction on PRI is small compared to the effect of atmospheric correction. However, the impact of surface reflectance anisotropy on a MODIS-based PRI is difficult to assess precisely. The standard MOD43 product only contains BRDF-parameters for the "land bands", i.e. the spectral bands 1–7. The theoretical benefit resulting from correcting anisotropy effects is eroded by the additional uncertainties caused by unavailability of BRDF shape parameters from the same day, location, and spectral bands as the radiance data. As considering BRDF effects is known to improve the quality of NDVI (Bacour et al., 2006), we used 6S in the BRDF-correction mode prior to the calculation of NDVI and EVI. The data set with no atmospheric correction applied was subject to the same constraints as for the 6S-approach to arrive at the same number of samples.

In the DOS-case reflectance was calculated as

$$\rho = \frac{\pi\left(L_{\text{sat}} - L_{\text{path}}\right)}{E_0 \cos(\Theta_z) T_z} \tag{5}$$

where L_{sat} is the at-satellite radiance, E_0 is the exoatmospheric solar constant (contained within MOD021km), and Θ_z is the solar zenith angle. T_z is the atmospheric transmittance in the illumination direction, fixed at 1 in this case. The path radiance is estimated separately for each spectral band as

$$L_{\text{path}} = L_{\text{sat,min}} - 0.01(E_0 \cos(\Theta_z) T_z) / \pi \tag{6}$$

The first step in retrieving L_{path} consisted in selecting all acquisition times when the pixel containing the tower is flagged as "confident clear", without cirrus clouds, heavy aerosol or shadows, and where the sensor zenith angle was no more than 40°. For scenes with flawless tower pixels the 25,000 pixels with the smallest Euclidean distance to the tower-pixel were examined for contamination by cloud cover, shadows, aerosols or bad detectors. $L_{\text{sat, min}}$ was then defined as the average of the 500 pixels with the lowest radiance among the good quality pixels neighbouring the tower pixel. A more detailed description of dark object subtraction can be found in Song et al. (2001).

The MODIS cloud mask does not allow the detection cloud cover or cloud shadows with absolute certainty. To rule these distortions out we only analysed at acquisition times where the diurnal curve of incident PAR (ground-based measurements) was near-perfect. We refer to this approach whenever we talk about cloud-free days in this study. The total screening left 439 acquisition times in case of the 6S approach (and "no correction") and 1145 acquisition times in case of the DOS approaches for further analysis. Due to increased cloud cover in winter the majority of usable image acquisitions occurs during the growing season.

2.3.2. Preparation of vegetation indices

In studies using field- or airborne spectrometers with high spectral resolution the PRI is defined as in Eq. (1). It is based on ρ_{531} (reflectance at 531 nm), which is sensitive to the epoxidation state of xanthophyll cycle pigments, and ρ_{570} (reflectance at 570 nm), being largely unaffected by short-term stress (Gamon et al., 1992).

MODIS-band 11 is centred at 531 nm (cf. Table 1). As the MODIS-sensor is not equipped with a spectral band centred at 570 nm, we tested bands 1 (620–670 nm), 4 (545–565 nm), 12 (546–556 nm), 13 low gain (662–672 nm), and 14 low gain (673–683 nm) as potential reference bands, in accordance with the proposition of Drolet et al.

(2005, 2008). To obtain only positive PRI-values that compare better with the traditional vegetation indices, a scaled PRI was calculated (Rahman, 2004):

$$\mathrm{sPRI} = (\mathrm{PRI} + 1)/2 \tag{7}$$

A modification of sPRI has been computed for each of the 5 reference bands and each of the 3 modes of atmospheric correction. To compare the performance of the PRI as a proxy of LUE against the capability of well known vegetation indices we calculated the normalised difference vegetation index (NDVI) (Tucker, 1979),

$$\mathrm{NDVI} = \frac{\rho_{\mathrm{NIR}} - \rho_{\mathrm{red}}}{\rho_{\mathrm{NIR}} + \rho_{\mathrm{red}}} = \frac{\rho_{\mathrm{bd2}} - \rho_{\mathrm{bd1}}}{\rho_{\mathrm{bd2}} + \rho_{\mathrm{bd1}}} \tag{8}$$

and the Enhanced Vegetation Index (EVI) (Huete et al., 1997),

$$\mathrm{EVI} = 2.5 \cdot \frac{\rho_{\mathrm{NIR}} - \rho_{\mathrm{red}}}{\rho_{\mathrm{NIR}} + 6 \cdot \rho_{\mathrm{red}} - 7.5 \cdot \rho_{\mathrm{blue}} + 1} \quad 2.5 \cdot \frac{\rho_{\mathrm{bd2}} - \rho_{\mathrm{bd1}}}{\rho_{\mathrm{bd2}} + 6 \cdot \rho_{\mathrm{bd1}} - 7.5 \cdot \rho_{\mathrm{bd3}} + 1} \tag{9}$$

from reflectance data that were corrected for atmospheric and BRDF effects.

2.4. Modelling GPP

In the end, we would like to know which approach of estimating light use efficiency gives the best results when modelling GPP with Eq. (2). The light use efficiency term will be approximated by (a) the VI that correlates best with LUE and (b) the LUE derived from the MODIS biome parameter look-up table and local temperature and VPD measurements. For (a) we applied leave-one-out cross-validation by fitting a linear model to all but one VI–LUE pairs. This model was then used to calculate a LUE value from the left-over VI value. This LUE estimate was then multiplied with the matching aPAR value: $\mathrm{GPP} = \mathrm{LUE} \cdot \mathrm{fAPAR} \cdot \mathrm{PAR} = (a \cdot \mathrm{VI} + b) \cdot \mathrm{FPAR} \cdot \mathrm{PAR}$. The relative difference of this modelled GPP value to the actually measured GPP was recorded. This procedure was repeated for every VI–LUE pair. For (a) we run one batch with reference LUE calculated as daily slope with only site data, for another batch we picked the LUE version with MODIS faPAR. With this cross-validation approach we reduced the risk of overfitting to the specific data available. We compared average values, mean absolute errors, and root mean squared error (RMSE). We used the modelling efficiency measure (ME, Janssen & Heuberger, 1995), which compares the relative improvement of the chosen model over the benchmark situation 'average of observed values':

$$\mathrm{ME} = 1 - \frac{\sum_{i=1}^{n}(O_i - M_i)^2}{\sum_{i=1}^{n}(O_i - \bar{O})^2} \tag{10}$$

We had a closer look at dry (soil water content <100 mm) and wet periods (soil water content >200 mm).

3. Results

3.1. Comparing LUEs at different time scales

Multiple good quality MODIS image acquisitions rarely occur on the same day for the same location. Even if, any light use efficiency that could be estimated from optical satellite data would still be a snapshot. The acquisition time can theoretically influence the ability to estimate daily LUE from satellite data. In summer time, the diurnal curve of GPP often displays a depression at midday, or GPP simply declines during midday and afternoon (data not shown). To check the effect of acquisition time on the estimation of daily LUE, we compared LUE calculated as half-hourly ratio against LUE calculated as daily ratio

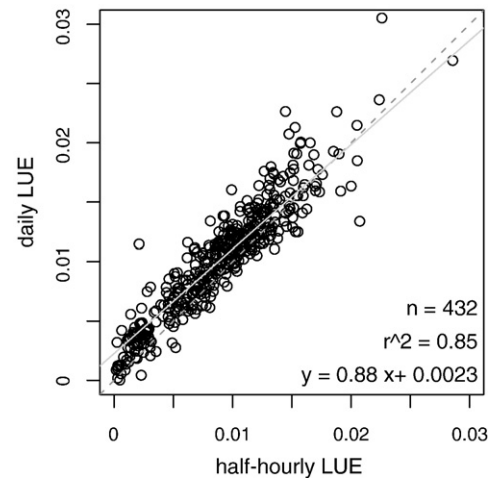

Fig. 2. Comparison of half-hourly and daily light use efficiency (LUE) for 12:00 to 12:30 at cloud free days (i.e. potential satellite acquisition days). Equally good or better relationships are observed for the other half-hour intervals between 10 a.m. and 2 p.m. The linear function fitted to the observations is shown by the continuous line, the 1:1 line is dashed.

for all cloud-free days of 2002–2005. The potential image acquisition times of the Aqua and Terra satellites in the study area range from 10 a.m. to 2 p.m. For all half-hour time steps within this interval the linear fit between daily and half-hourly LUE yielded a correlation coefficient of at least 0.92 ($p<0.001$, example for 12:00 to 12:30 shown in Fig. 2). The linear functions relating the half-hourly and the daily LUE in each time interval are close to the 1:1 line (slope 0.86–0.97, intercept 0.0013–0.0023).

The relative similarity of half-hourly and daily LUEs is also revealed on an annual basis. While-naturally-some half-hourly LUEs exceed the daily LUE, the annual means are comparable and display the same interannual variations (Fig. 3A). The 90th percentile of daily LUE ranges between 0.0261 (2002) and 0.0230 μmol CO_2/μmol photons (2002); this difference is equivalent to 11% of the 2002 value. The 90th percentiles of all years exceed the maximum LUE given in the MODIS biome property look-up table (BPLUT) for evergreen broadleaf forests (0.021 μmol CO_2/μmol photons). The LUE calculated according to the MODIS GPP algorithm does about represent the average LUE in non-summer months. However, during the summer months, a decline in LUE calculated from site GPP and aPAR can be observed that is not captured by BPLUT-based LUE (Fig. 3).

3.2. Strength of relationship between VIs and LUE, aPAR, and GPP

We then checked the correlation between 14 varieties of LUE and the vegetation indices, i.e. the sPRI with 5 different reference wavelength and 3 modes of atmospheric correction each, as well as the NDVI, and EVI. For each viewing-geometry constrained subset of observations we made sure that all VIs were available simultaneously. Whether we look at the full data set or constrain to certain sun-sensor geometries: the behaviour of LUE in the family of ratios at daily and sub-daily level is very consistent. Therefore only one representative is displayed in Fig. 4A–E. In our study, the PRI with the broad reference band 1 yielded the best correlation with ecosystem LUE (r up to 0.78). However, we only achieved such a good correlation when constraining the dataset with respect to viewing geometry and when we did not apply atmospheric correction. In the following we will detail the effects of different constraints.

Looking at the whole dataset, only constrained as outlined in Section 2 (Fig. 4A), we find that the scaled PRI with the red reference bands (1, 13, 14) correlate best with the ground based LUE estimates ($r=0.65$, $p<0.001$ for LUE calculated with MODIS faPAR, $n=156$ samples). Choosing only observations made by either Terra or Aqua does

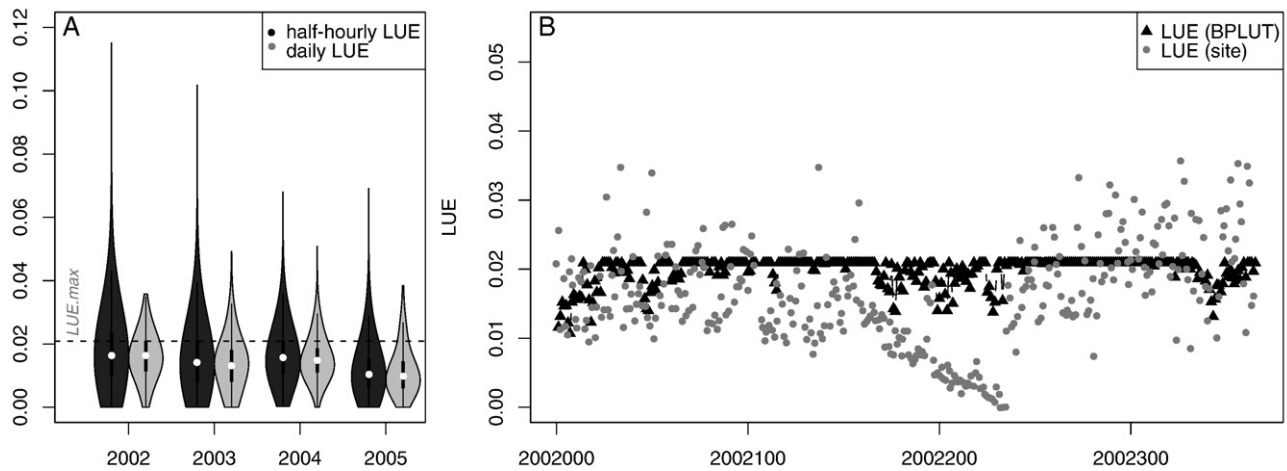

Fig. 3. (A) Annual means and standard deviation of half-hourly and daily light use efficiency; LUE.max: maximum LUE for evergreen broadleaf forests according to MOD17 biome property look-up table (BPLUT) (B) BPLUT-approach does not capture LUE dynamics of the site, similar pattern for all years.

change neither the strength of the correlation nor the slope of a linear function fitted to the LUE and PRI values (data not shown). The best relationship between a "traditional vegetation index" and LUE is $r \leq 0.43$, for NDVI with atmospheric (Lambertian) correction ($p < 0.001$). For all sPRIs analysed, none of the atmospheric correction procedures tested does yield a significantly better correlation with LUE compared to sPRI calculated from top-of-atmosphere reflectances.

As a next step we only look at satellite data that are subject to backscatter conditions, that is to say where sun and sensor have $\leq 10°$ difference in zenith angle and $\leq 60°$ difference in azimuth angle. Because of these constraints and because we made sure that we compared vegetation indices from exactly the same observation times, only six samples remained. For these 6 days, correlation between the remaining sPRI and LUE values does improve a lot (data not shown because of sample size). sPRI with reference band 14 yields the best correlation with LUE ($r = 0.91$, for LUE based on MODIS faPAR, followed by sPRI with reference bands 13 and 1. For observations near backscatter direction atmospheric correction seems to be necessary to obtain a good relationship between the different sPRIs and LUE. Due to the small number of observations in this configuration we must be careful not to attach too much importance to this result. Neither NDVI nor EVI have a correlation with LUE to speak of.

Constraining the satellite data to sensor zenith angles (SZA) of $\leq 10°$) or 30–40° increases the correlation between LUE and all vegetation indices compared to the complete data set (Fig. 4B, E). The sPRI with reference bands 1, 13, and 14 perform similarly well regarding their correlation with LUE (r up to 0.79 for sPRI with reference band 1 and LUE based on MODIS faPAR, no atmospheric correction, $p < 0.001$). In the subsets with 10–20° and 20–30° SZA the correlation between vegetation indices and LUE is comparable to the full data set, both in pattern and magnitude. For the viewing angle restricted data sets atmospheric correction does generally not improve the correlation. NDVI and PRI with reference band 1 at near-nadir SZA are the only exceptions.

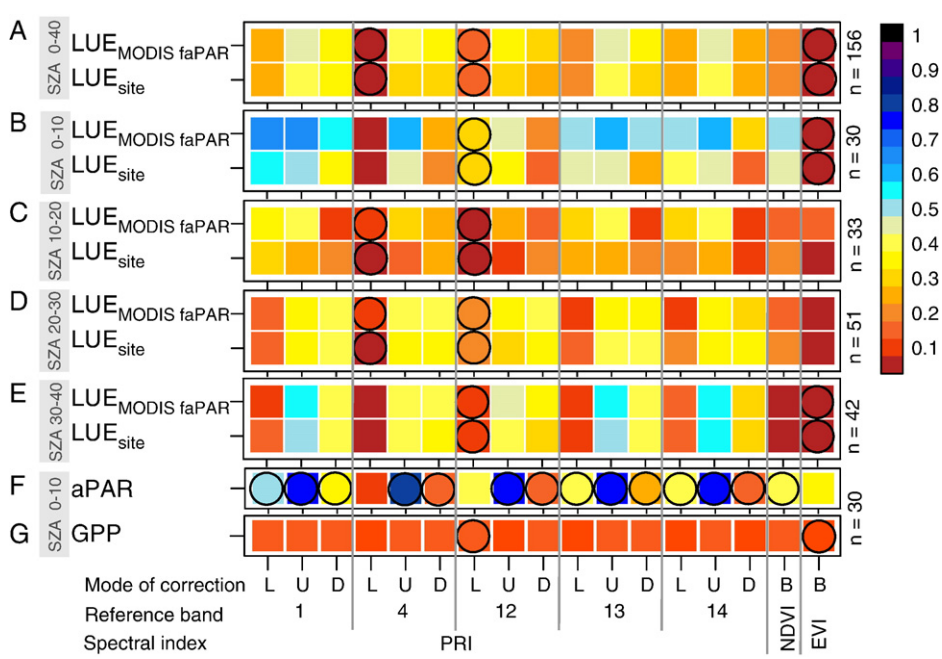

Fig. 4. (A–E) Correlation between ground based light use efficiency estimates (LUE with faPAR from MODIS data and from interception measurements, c.f. Section 2) and MODIS vegetation indices. (A) Sensor zenith angle (SZA) 0–40°, (B) SZA 0–10°, (C) SZA 10–20°, (D) SZA 20–30°, and (E) SZA 30–40°. (F) Correlation of aPAR and VI. (G) Correlation of GPP and VI (F–G) constraints as for B. Black circles indicate negative correlation. The atmospheric correction modes are abbreviated with L (correction with 6S assuming Lambertian conditions), B (correction with 6S considering BRDF effects), U (uncorrected), and D (dark object subtraction).

On the whole, PRI without atmospheric correction correlates best with LUE. This pattern shows up again when correlating the VIs with absorbed PAR. The uncorrected sPRIs show a strong relationship with aPAR, this time negative (example for 0–10° SZA shown in Fig. 4F). The correlation patterns of other LUE variations versus VIs do also correspond to the aPAR correlation patterns, albeit at a lower magnitude and only after selecting for narrow SZA (not all data shown). We observe no correlation between GPP and sPRI or the other VIs (Fig. 4G). This pattern is consistent regardless of the constraints applied to the data set.

3.3. Ability of sPRI to track LUE over time

The sPRI with reference band 1(as well as the two narrow red bands) and no atmospheric correction (SZA 0–10°) does well in tracking the seasonal course of light use efficiency (Fig. 5A). Especially, it picks up the decline in LUE during drought periods in the summer (Fig. 5C). The best performing sPRI (reference band 1, no atmospheric correction, SZA 0–10°) yields a somewhat higher correlation with LUE than the best performing traditional vegetation index (NDVI, reflectances corrected with 6S assuming Lambertian behaviour, SZA 0–10°), that is $r=0.78$, $p<0.001$ compared to $r=0.70$, $p<0.001$ (Fig. 4). This relationship deteriorates when all available data in this range of SZA are considered, not only those where all vegetation indices are available simultaneously (Fig. 5). EVI is a far worse predictors of LUE. The PRI (and LUE) is minimal during summer droughts. Since the amount of incident PAR is maximum in summer, aPAR and PRI are inversely correlated ($r=-0.86$, $p<0.001$) for sPRI with reference band 1, no atmospheric correction, SZA 0–10° and daily aPAR; c.f. Fig. 4). All of the potential reference bands tested in this study are clearly influenced by the same forcing and show a distinct seasonal cycle. The changes within the ecosystem add to the effects caused for instance by viewing geometry and absorbed PAR and can be visualised as normalised ratios. As band 1 integrates over the wavelength of bands 13 and 14 it is not surprising that they show the same temporal variation. The gaps in summertime result from saturation of the narrow red bands. These bands were designed with a higher sensitivity to monitor dark oceanic surfaces and are thus more likely to saturate

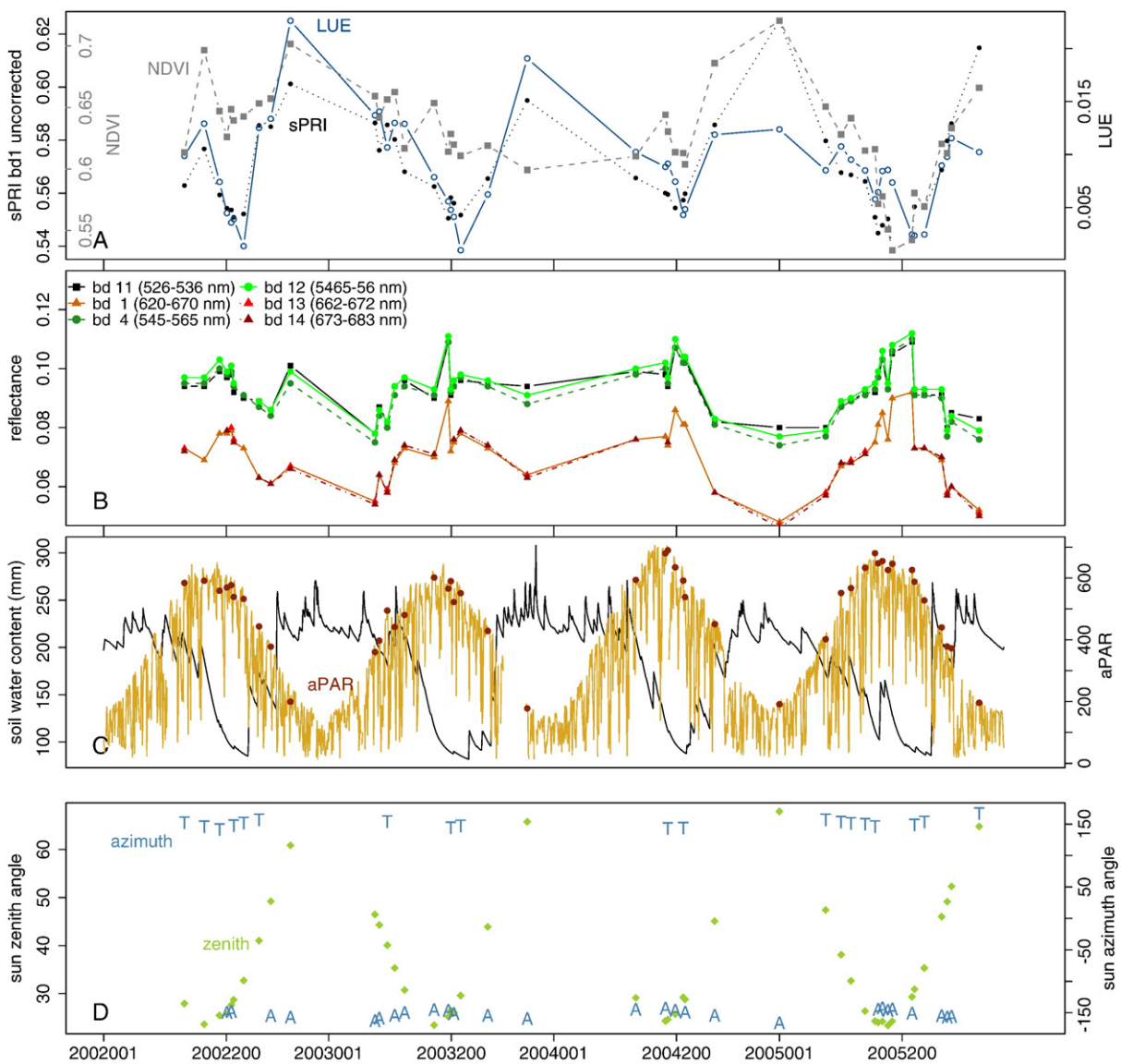

Fig. 5. (A) Time series of LUE, best-performing PRI (reference band 1, no radiance correction), and best-performing other vegetation index (NDVI with BRDF correction). (B) Reflectances used for PRI calculation (no atmospheric correction) (A + B). Only observations with near-nadir viewing angles are shown. (C) Cumulative water deficit as water stress indicator and daily aPAR averages. (D) Sun zenith and azimuth angles during time of image acquisition (A + C). A = Aqua, T = Terra.

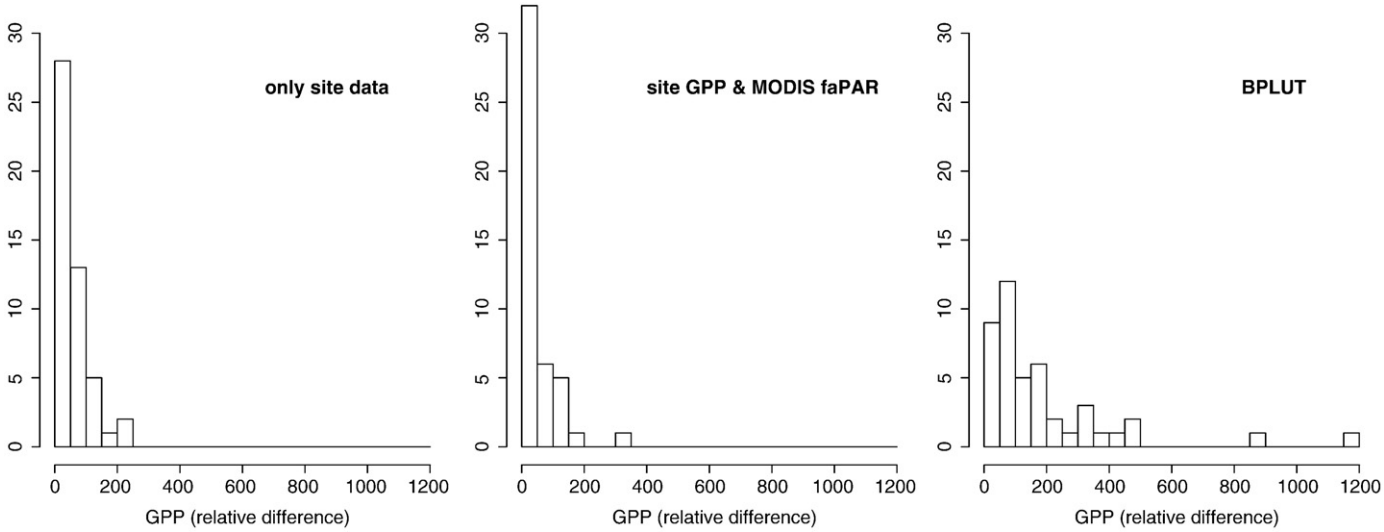

Fig. 6. Relative difference (%) between observed GPP and GPP derived from n light use efficiency models. The LUE for the two leftmost models was estimated from sPRI (reference band 1, no atmospheric correction, SZA 0–10°), based on a regression of the other $n-1$ sPRI values against LUE estimates. In the right-hand model, LUE is calculated from MODIS biome property look-up table (BPLUT) parameters and site meteorological data.

over relatively bright terrestrial targets, especially when vegetation cover is not dense.

3.4. Modelling GPP

The VI selected as LUE-proxy in this analysis is the sPRI with reference band 1 and no atmospheric correction performed (constrained to near nadir viewing angles). PRI with reference band 1 was chosen over the PRIs with reference bands 13 and 14 because band 1 does rarely saturate and thus yields a higher data coverage. As shown in Section 3, the PRIs with red reference bands otherwise behave very similar. Setting up a model with this sPRI and a site-data-only LUE yields a relative difference between modelled and observed GPP of 40.2% (median, $n=49$, c.f. Fig. 6, Table 2). When the GPP estimation is based on LUE with MODIS faPAR, the difference to the observed GPP is 50.6% (median, $n=44$). If GPP is modelled with the MODIS algorithm, the difference to the observed GPP is as large as 151% (median). To achieve comparability, we chose the same observation times as in the first set-up ($n=49$). With the look-up table approach GPP is severely overestimated during all satellite data acquisition times (near nadir viewing angles) and even more so during times of water stress (Table 3). In contrast, the discrepancy between observed GPP values and PRI-based GPP estimates during dry periods is not much different from periods with high water availability.

Table 2
Comparison of GPP-models (c.f. Section 4).

	LUE from		
	Site data only	Site GPP and MODIS faPAR	BPLUT
Number of obs.	49	45	44
Avg. modelled GPP*	2.126	3.860	8.747
Avg. observed GPP*	3.981	4.051	4.047
Mean absolute error*	2.088	1.390	4.752
RMSE*	2.3208	3.389	27.345
Modelling efficiency	$-5.172\cdot10^{32}$	$-1.034\cdot10^{30}$	$-3.470\cdot10^{32}$

The LUE for the two leftmost models was estimated from sPRI (reference band 1, no atmospheric correction, sensor zenith angle 0–10°), based on a regression of the other $n-1$ sPRI values against LUE estimates. In the model on the right, LUE is calculated from MODIS biome property look-up table (BPLUT) parameters and site meteorological data. Numbers are dimensionless or in μmol CO_2 m^{-2} s^{-1} (*).

4. Discussion

4.1. Comparing LUEs at different time scales

We demonstrate specifically for a water-limited site that midday LUE on cloud-free days is a good proxy for daily LUE (Fig. 2). Other experimental evidence suggests that this relationship might be generally applicable. Sims et al. (2005) report a good relationship between midday and daily LUE on clear days ($r=0.85$) for pooled data from a wide range of vegetation types. This was indirectly confirmed for a boreal deciduous forest where Drolet et al. (2005) found low variability in LUE on days useful for MODIS image acquisition. In this case, faPAR for LUE calculation was derived from tower measurements of NDVI. For pooled data from a Canadian boreal forest with different plant functional types and levels of disturbance, Drolet et al. (2008) found a strong relationship between midday and daily LUE ($r=0.96$) on clear days (using MODIS faPAR). That we do not find strong differences in the PRI–LUE relationship for different LUE aggregation levels does fit in with this general picture.

The highest 90th percentile of daily LUE per year within the study period amounted to 0.0261 (2002). This compares well with the maximum LUE in other semiarid ecosystems, for instance Sims et al. (2006) reported a maximum daily LUE of 0.02 for a relatively sparse Californian chaparral ecosystem. The site specific maximum LUE is subject to considerable interannual variability (Fig. 3). Within the 4

Table 3
Average difference between observed and modelled GPP (cf. Section 4, Table 2) in dry periods, well-watered periods, and the whole time series with standard deviation (in μmol CO_2 m^{-2} s^{-1}).

LUE from	ΔGPP_{dry}	ΔGPP_{wet}	ΔGPP_{all}
Site data only	1.602 ± 1.239 (14)	1.107 ± 1.995 (11)	1.855 ± 1.955 (49)
Site GPP and MODIS faPAR	-0.120 ± 1.276 (14)	-0.142 ± 1.366 (11)	0.191 ± 1.852 (45)
BPLUT	-6.230 ± 1.443 (14)	-2.598 ± 2.481 (10)	-4.596 ± 2.396 (44)

In parentheses: number of observations.

years analysed, the 90th percentile varied by 11%. This indicates that MOD17-like models might improve their performance if parameters were optimised on an annual basis. The operational MOD17 maximum LUE for evergreen broadleaf forests was too low for the Puéchabon forest in the study period. Moreover, the MOD17 biome property look-up table (BPLUT) approach did not simulate the summer depression in LUE, although we used accurate on-site measurements of temperature and VPD. In principle, an optimisation of the MOD17 BPLUT parameters could reduce the discrepancy between modelled and actual LUE. In any case, the error in MOD17 GPP is likely to increase when the constraining environmental factors are extracted from global meteorology datasets. Also, for this particular site the complete water balance needs to be considered to model GPP accurately (unpublished results by Markus Reichstein). Considering soil water content might theoretically improve the situation but retrieving (deep) soil moisture on large spatial scales is not feasible. These results justify the search for alternative LUE estimates.

4.2. Strength of relationship between VIs and LUE, aPAR, and GPP

In this study, the red MODIS spectral bands (620–670 nm, 662–672 nm, 673–683 nm) turned out to be the most suitable reference bands for PRI (Fig. 4). The PRI with red reference bands was shown to be clearly more related to LUE than NDVI or EVI. This behaviour is as expected, it has been shown before that using NDVI results in an overestimation of productivity, especially in water limited sites (Running & Nemani, 1988). When sampling the total set of satellite data for acquisitions within a narrow range of viewing angles, we found stronger relationships between all versions of PRI and LUE compared to the complete data set. This is especially true for near-nadir viewing angles and viewing zenith angles of 30–40°. Barton and North (2001) showed in a simulation study that the influence of soil background reflectance on PRI is significant for canopies with a LAI below 3. The relatively sparse vegetation cover in the study area (LAI just below 3) might thus give rise to a sensitivity of the PRI–LUE relationship to differences in viewing angle. We also need to keep in mind that the PRI, since it is observed from above, represents at best top-of-canopy conditions, not an average over the whole canopy. Some scatter in the LUE–PRI relationship is probably due to this fundamental difference between any optical remote sensing data and the eddy covariance based GPP estimates involved in the evaluation, which integrate over the whole canopy.

For a boreal deciduous forest (Drolet et al., 2005) found a strong linear positive relationship between LUE and PRI with reference band 13 calculated from backscatter top-of-atmosphere reflectance ($r=0.87$). A weaker relationship was found when using reference band 12 ($r=0.73$). They found no significant correlation for the reference bands 1 and 4. Drolet et al. (2008) estimated ecosystem LUE for several Canadian boreal forest sites with different plant functional types and degrees of disturbance with MODIS bands 10, 12, 13, and 14 (488 nm, 551 nm, 667 nm, and 678 nm) as reference bands. Reference band 14 yielded the best correlation with LUE ($r^2=0.70$, pooled data). However, in that study no significant correlation was observed for the individual sites. In our study, PRIs formed with the narrow red bands 13 and 14 have about the same relationship to LUE as a PRI with the broader red band 1 (c.f. Fig. 4). Red might be generally useful as a reference band for MODIS based PRI.

Garbulsky et al. (2008) estimated LUE of an Italian *Quercus ilex* forest (LAI = 3.5) with a MODIS-based PRI. Using at-sensor-radiance and band 12 for reference they found a good correlation ($r=0.78$) for all cloud-free image acquisition days. The better performance of reference band 12 and the lower sensitivity to viewing geometry compared to the Puéchabon site might be due to the higher LAI (3.5 compared to 2.8 ± 0.4), and maybe also due to generally better water availability (Reichstein et al., 2002). The performance of the red bands at this closed-canopy stand was not published. For using a satellite-derived PRI at larger spatial scales it will be necessary to find out the optimal reference band under different conditions. If no universally applicable reference band can be identified, we would need to establish stratification rules.

In this study using top-of-atmosphere reflectance data for PRI calculation yielded the highest correlation with LUE for most viewing geometries. In the backscatter constellation, correction with 6S was better, although based on few data. Drolet et al. (2005) reported a similar phenomena. This suggests that the estimates of atmospheric optical thickness provided as MODIS product and/or atmospheric correction with 6S add uncertainty to the small PRI signal. The sampling frequency and the range of viewing angles used to produce the MODIS atmospheric optical thickness product might be a limiting factor. Integrating data from other satellite missions might mitigate this problem. The simulation study performed by Barton and North (2001) suggests that the index is robust to variation in aerosol as the top-of-atmosphere PRI followed the ground PRI over a range of optical thickness. Their explanation is that the (original) bands are close in wavelength and so unlike Rayleigh scattering the aerosol effects are similar at both 531 and 570 nm. This reasoning is not so convincing when using a red reference band. Currently, we do not have an explanation why using uncorrected red bands gives nevertheless the best results.

4.3. Ability of sPRI to track LUE over time

The MODIS-based PRI with one of the reference bands 1, 13, or 14 and no radiance correction applied is able to track the seasonal course of LUE if the observations are constrained to narrow ranges of viewing angles. It is the first time this has been demonstrated for a severely water limited Mediterranean site. The constraints in viewing geometry probably limit the effect of anisotropy in surface reflectance. The remaining temporal variations in the PRI signal in the restricted data sets are better linked with variations in ecosystem LUE. It is likely that not only the xanthophyll-cycle pigment interconversions give raise to the changes in PRI but also seasonal changes in the concentration of xanthophyll cycle pigments. Xanthophyll levels, carotenoid concentrations in general, and chlorophyll levels relate to seasonal changes in vegetation productivity; the PRI signal has been shown to match these variations (Sims & Gamon, 2002; Sims et al., 2006; Stylinski et al., 2002). Filella et al. (2004) state that xanthophyll and carotenoid levels change with environmental conditions and thus also are indicators of photosynthetic downregulation under stress.

The NDVI did not track the decline in LUE as well as the PRI with reference band 1 (Fig. 5). Sims et al. (2006) gave one plausible explanation for this: compared to PRI the NDVI seasonal pattern is more sensitive to solar elevation angle effects. The relatively good correspondence between NDVI and LUE in the summer of 2005 compared to previous summers probably results from a caterpillar attack (Allard et al., 2008).

Gamon et al. (1992) tried different reference wavelength for sunflower canopies, 550 nm did not work well with the water stress experiments. Leaves of sclerophylly are less prone to wilting, hence the fraction of soil seen from sensor does not vary (due to wilting, but surely due to changes in viewing angle).

4.4. Modelling GPP

In this study, GPP models relying on PRI as an LUE proxy yielded considerably more agreement with observations than the MODIS GPP algorithm, especially during dry periods. Both approaches were tested with site meteorological data (including incPAR) and MODIS faPAR, hence the differences in performance are not due to the quality of input data. Further research should address the performance of PRI based models with a more universal parameterisation (e.g. for all Mediterranean evergreen needleleaf forests).

Data from optical sensors such as MODIS are often cloud contaminated, temporal aggregations are used to increase the spatial coverage. Sims et al. (2005) documented that the inclusion of cloudy days leads to a large variation of LUE within the aggregation period and thus disturbs the relationship between midday LUE and LUE of the aggregation period. They suggest to estimate midday LUE from satellite data and to compute midday gross carbon fluxes from that. Then rather robust relationships between midday gross carbon flux and eight-day fluxes should be used to extrapolate to longer time periods.

4.5. General considerations

Overall, the Puéchabon *Quercus ilex* forest seems to be a suitable test case to study the performance of satellite based PRI in drought-prone areas. For this evergreen forest the PRI signal is not dominated by large seasonal variations in leaf area through senescence or strong wilting. Other semiarid ecosystems, for instance those with brevi-deciduous leaves and sparser canopy structure, can be less suitable for PRI studies (Filella et al., 2004; Sims et al., 2006). But also for the sclerophylly site studied here we can not exclude that the relationship between PRI and LUE in years with excessive drought might differ from years with normal droughts. Sims et al. (2006) observed such changes for a Californian chaparral ecosystem.

5. Conclusions

We found that MODIS PRI seems to be a useful estimator of ecosystem LUE, despite the influence of soil and other photosynthetically inactive material on the reflectance signal. This statement is valid during the whole growing season and also times of severe water deficiency. The light use efficiency at times of satellite data acquisition is close to the daily average of light use efficiency, thus PRI can be used to estimate daily LUE. The PRI with either of the three tested red reference bands is correlated best with on-site LUE. Given that the narrow red bands 13 and 14 are prone to saturation in summer and thus provide less useful observations, band 1 seems to be the best reference band for the evergreen oak forest studied here. Since the choice of reference band matters, we recommend to perform an independent careful screening for each new study area, or to look for a universally applicable reference band for MODIS-based PRI. NDVI and EVI were comparatively poor proxies of LUE. The relationship between PRI and LUE improves when the analysis is restricted to small ranges of viewing angles. Near nadir viewing angles yield the best results. In the end, this study also demonstrates that GPP models relying on PRI as a LUE proxy correspond considerably better with observations than the MODIS GPP algorithm, especially when water is scarce.

Acknowledgements

We would like to acknowledge the comments made by the anonymous reviewers of this paper. They helped to improve the clarity of the manuscript considerably. We are also grateful for discussions with François-Marie Bréon.

References

Allard, V., Ourcival, J., Rambal, S., Joffre, R., & Rocheteau, A. (2008). Seasonal and annual variation of carbon exchange in an evergreen Mediterranean forest in southern France. *Global Change Biology*, *14*(4), 714—725.

Bacour, C., Bréon, F., & Maignan, F. (2006). Normalization of the directional effects in NOAA-AVHRR reflectance measurements for an improved monitoring of vegetation cycles. *Remote Sensing of Environment*, *102*(3–4), 402—413.

Barton, C., & North, P. (2001). Remote sensing of canopy light use efficiency using the photochemical reflectance index — Model and sensitivity analysis. *Remote Sensing of Environment*, *78*(3), 264—273.

Christensen, J., Hewitson, B., Busuioc, A., Chen, A., Gao, X., Held, I., et al. (2007). Regional climate projections. Climate change 2007: The physical science basis. *Contribution of Working Group I to the Fourth assessment report of the intergovernmental panel on climate change* (p. 94).

Clausi, D. (2002). An analysis of co-occurrence texture statistics as a function of grey level quantization. *Canadian Journal of Remote Sensing*, *28*(1), 45—62.

Demmig-Adams, B., & Adams, W. (2006). Photoprotection in an ecological context: The remarkable complexity of thermal energy dissipation. *New Phytologist*, *172*(1), 11—21.

Demmig, B., Winter, K., Krüger, A., & Czygan, F. -C. (1987). Photoinhibition and zeaxanthin formation in intact leaves: A possible role of the xanthophyll cycle in the dissipation of excess light energy. *Plant Physiology*, *84*(2), 218—224.

Drolet, G., Huemmrich, K., Hall, F., Middleton, E., Black, T., Barr, A., et al. (2005). A MODIS-derived photochemical reflectance index to detect inter-annual variations in the photosynthetic light-use efficiency of a boreal deciduous forest. *Remote Sensing of Environment*, *98*(2–3), 212—224.

Drolet, G., Middleton, E., Huemmrich, K., Hall, F., Amiro, B., Barr, A., et al. (2008). Regional mapping of gross light-use efficiency using MODIS spectral indices. *Remote Sensing of Environment*, *90*(3), 308—318.

Filella, I., Penuelas, J., Llorens, L., & Estiarte, M. (2004). Reflectance assessment of seasonal and annual changes in biomass and CO_2 uptake of a Mediterranean shrubland submitted to experimental warming and drought. *Remote Sensing of Environment*, *90*(3), 308—318.

Galmés, J., Medrano, H., & Flexas, J. (2007). Photosynthetic limitations in response to water stress and recovery in Mediterranean plants with different growth forms. *New Phytologist*, *175*(1), 81—93.

Gamon, J., Field, C., Bilger, W., Bjoerkman, O., Fredeen, A., & Penuelas, J. (1990). Remote sensing of the xanthophyll cycle and chlorophyll fluorescence in sunflower leaves and canopies. *Oecologia*, *85*(1), 1—7.

Gamon, J., Field, C., Goulden, M., Griffin, K., Hartley, A., Joel, G., et al. (1995). Relationships between NDVI, canopy structure, and photosynthesis in 3 Californian vegetation types. *Ecological Applications*, *5*(1), 28—41.

Gamon, J., Fillela, I., & Penuelas, J. (1993). The dynamic 531-nm reflectance signal: A survey of twenty angiosperm species. In H. Y. Yamamoto & C. S. (Eds.), *Photosynthetic responses to the environment* (pp. 172—177). Rockville: American Society of Plant Physiologists.

Gamon, J., Penuelas, J., & Field, C. (1992). A narrow-waveband spectral index that tracks diurnal changes in photosynthetic efficiency. *Remote Sensing of Environment*, *41*(1), 35—44.

Garbulsky, M., Penuelas, J., Papale, D., & Filella, I. (2008). Remote estimation of carbon dioxide uptake by a Mediterranean forest. *Global Change Biology*, *14*, 1—8.

Giorgi, F. (2006). Climate change hot-spots. *Geophysical Research Letters*, *33*(8), L08707.

Goeckede, M., Foken, T., Aubinet, M., Aurela, M., Banza, J., Bernhofer, C., et al. (2008). Quality control of CarboEurope flux data – Part 1: Coupling footprint analyses with flux data quality assessment to evaluate sites in forest ecosystems. *Biogeosciences*, *5*(2), 433—450.

Goetz, S., Prince, S., Goward, S., Thawley, M., Small, J., & Johnston, A. (1999). Mapping net primary production and related biophysical variables with remote sensing: Application to the BOREAS region. *Journal of Geophysical Research*, *104*(D22), 27719—27734.

Gower, S., Kucharik, C., & Norman, J. (1999). Direct and indirect estimation of leaf area index, f(APAR), and net primary production of terrestrial ecosystems. *Remote Sensing of Environment*, *70*(1), 29—51.

Grace, J., Nichol, C., Disney, M., Lewis, P., Quaife, T., & Bowyer, P. (2007). Can we measure terrestrial photosynthesis from space directly, using spectral reflectance and fluorescence? *Global Change Biology*, *13*(7), 1484—1497.

Green, D., Erickson, J., & Kruger, E. (2003). Foliar morphology and canopy nitrogen as predictors of light-use efficiency in terrestrial vegetation. *Agricultural and Forest Meteorology*, *115*(3–4), 165—173.

Heinsch, F., Reeves, M., Votava, P., Kang, S., Milesi, C., Zhao, M., et al. (2003). User's guide: GPP and NPP (MOD17A2/A3) products. NASA MODIS land algorithm. *Version 2.0. Tech. rep., MODIS Land Team*.

Heinsch, F., Zhao, M., Running, S., Kimball, J., Nemani, R., Davis, K., et al. (2006). Evaluation of remote sensing based terrestrial productivity from MODIS using regional tower eddy flux network observations. *IEEE Transactions on Geoscience and Remote Sensing*, *44*(7), 1908—1925.

Huete, A., Liu, H., Batchily, K., & vanLeeuwen, W. (1997). A comparison of vegetation indices global set of TM images for EOS-MODIS. *Remote Sensing of Environment*, *59*(3), 440—451.

Janssen, P., & Heuberger, P. (1995). Calibration of process-oriented models. *Ecological Modelling*, *83*(1–2), 55—66.

Kumar, M., & Monteith, J. (1981). Remote sensing of crop growth. In H. Smith (Ed.), *Plants and the daylight spectrum* (pp. 133—144). New York: Academic Press.

Lacaze, B., Rambal, S., & Winkel, T. (1994). Identifying spatial patterns of Mediterranean landscapes from geostatistical analysis of remotely sensed data. *International Journal of Remote Sensing*, *15*(12), 2437—2450.

Leuning, R., Cleugh, H., Zegelin, S., & Hughes, D. (2005). Carbon and water fluxes over a temperate *Eucalyptus* forest and a tropical wet/dry savanna in Australia: Measurements and comparison with MODIS remote sensing estimates. *Agricultural and Forest Meteorology*, *129*(3–4), 151—173.

Martel, M., Margolis, H., Coursolle, C., Bigras, F., Heinsch, F., & Running, S. (2005). Decreasing photosynthesis at different spatial scales during the late growing season on a boreal cutover. *Tree Physiology*, *25*(6), 689—699.

Meroni, M., Rossini, M., Picchi, V., Panigada, C., Cogliati, S., Nali, C., et al. (2008). Assessing steady-state fluorescence and PRI from hyperspectral proximal sensing as early indicators of plant stress: The case of ozone exposure. *Sensors*, *8*(3), 1740—1754.

Monteith, J. (1972). Solar radiation and productivity in tropical ecosystems. *Journal of Applied Ecology*, *9*(3), 747—766.

Monteith, J. (1977). Climate and efficiency of crop production in Britain. *Philosophical Transactions of the Royal Society of London. Series B, Biological Sciences*, *281*(980), 277—294.

Myneni, R., Hoffman, S., Knyazikhin, Y., Privette, J., Glassy, J., Tian, Y., et al. (2002). Global products of vegetation leaf area and fraction absorbed PAR from year one of MODIS data. *Remote Sensing of Environment*, *83*(1–2), 214—231.

Naumann, J., Young, D., & Anderson, J. (2008). Leaf chlorophyll fluorescence, reflectance, and physiological response to freshwater and saltwater flooding in the evergreen shrub, *Myrica cerifera*. *Environmental and Experimental Botany*, *63*(1–3), 402—409.

Nichol, C., Huemmrich, K., Black, T., Jarvis, P., Walthall, C., Grace, J., et al. (2000). Remote sensing of photosynthetic-light-use efficiency of boreal forest. *Agricultural and Forest Meteorology*, *101*(2–3), 131—142.

Nichol, C., Lloyd, J., Shibistova, O., Arneth, A., Roser, C., Knohl, A., et al. (2002). Remote sensing of photosynthetic-light-use efficiency of a Siberian boreal forest. *Tellus B*, *54*(5), 677—687.

Papale, D., Reichstein, M., Aubinet, M., Canfora, E., Bernhofer, C., Kutsch, W., et al. (2006). Towards a standardized processing of Net Ecosystem Exchange measured with eddy covariance technique: Algorithms and uncertainty estimation. *Biogeosciences*, *3*(4), 571—583.

Penuelas, J., Filella, I., & Gamon, J. (1995). Assessment of photosynthetic radiation use efficiency with spectral reflectance. *New Phytologist*, *131*(3), 291—296.

Quézel, P., & Médail, F. (2003). *Ecologie et biogeographie des forêts du bassin méditerranéenne*. Elsevier.

Rahman, A. (2004). Potential of MODIS ocean bands for estimating CO_2 flux from terrestrial vegetation: A novel approach. *Geophysical Research Letters*, *31*(10), 4.

Rambal, S. (1993). The differential role of mechanisms for drought resistance in a Mediterranean evergreen shrub: A simulation approach. *Plant, Cell and Environment*, *16*(1), 35—44.

Rebmann, C., Göckede, M., Foken, T., Aubinet, M., Aurela, M., Berbigier, P., et al. (2005). Quality analysis applied on eddy covariance measurements at complex forest sites using footprint modelling. *Theoretical and Applied Climatology*, *80*(2–4), 121—141.

Reichstein, M., Falge, E., Baldocchi, D., Papale, D., Aubinet, M., Berbigier, P., et al. (2005). On the separation of net ecosystem exchange into assimilation and ecosystem respiration: Review and improved algorithm. *Global Change Biology*, *11*(9), 1424—1439.

Reichstein, M., Tenhunen, J., Roupsard, O., Ourcival, J., Rambal, S., Miglietta, F., et al. (2002). Severe drought effects on ecosystem CO_2 and H_2O fluxes at three Mediterranean evergreen sites: Revision of current hypotheses? *Global Change Biology*, *8*(10), 999—1017.

Ruimy, A., Saugier, B., & Dedieu, G. (1994). Methodology for the estimation of terrestrial net primary production from remotely sensed data. *Journal of Geophysical Research*, *99*(D3), 5263—5283.

Running, S., & Nemani, R. (1988). Relating seasonal patterns of the AVHRR vegetation index to simulated photosynthesis and transpiration of forests in different climates. *Remote Sensing of Environment*, *24*(2), 347—367.

Runyon, J., Waring, R., Goward, S., & Welles, J. (1994). Environmental limits on net primary production and light-use efficiency across the Oregon Transect. *Ecological Applications*, *4*(2), 226—237.

Schwalm, C., Black, T., Arniro, B., Arain, M., Barr, A., Bourque, C. -A., et al. (2006). Photosynthetic light use efficiency of three biomes across an east–west continental-scale transect in Canada. *Agricultural and Forest Meteorology*, *140*(1–4), 269—286.

Sims, D., & Gamon, J. (2002). Relationships between leaf pigment content and spectral reflectance across a wide range of species, leaf structures and developmental stages. *Remote Sensing of Environment*, *81*(2–3), 337—354.

Sims, D., Luo, H., Hastings, S., Oechel, W., Rahman, A., & Gamon, J. (2006). Parallel adjustments in vegetation greenness and ecosystem CO_2 exchange in response to drought in a Southern California chaparral ecosystem. *Remote Sensing of Environment*, *103*(3), 289—303.

Sims, D., Rahman, A., Cordova, V., Baldocchi, D., Flanagan, L., Goldstein, A., et al. (2005). Midday values of gross CO flux and light use efficiency during satellite overpasses can be used to directly estimate eight-day mean flux. *Agricultural and Forest Meteorology*, *131*(1–2), 1—12.

Song, C., Woodcock, C., Seto, K., Lenney, M., & Macomber, S. (2001). Classification and change detection using Landsat TM data: When and how to correct atmospheric effects? *Remote Sensing of Environment*, *75*(2), 230—244.

Stylinski, C., Gamon, J., & Oechel, W. (2002). Seasonal patterns of reflectance indices, carotenoid pigments and photosynthesis of evergreen chaparral species. *Oecologia*, *131*(3), 366—374.

Suarez, L., Zarcotejada, P., Sepulcrecanto, G., Perezpriego, O., Miller, J., Jimenezmunoz, J., et al. (2008). Assessing canopy PRI for water stress detection with diurnal airborne imagery. *Remote Sensing of Environment*, *112*(2), 560—575.

Terradas, J. (1999). Holm oak and holm oak forests: An introduction. In F. Roda (Ed.), *Ecology of Mediterranean evergreen forestsEcological Studies*, *Vol. 137*. (pp. 3—14) Springer.

Tucker, C. (1979). Red and photographic infrared linear combinations for monitoring vegetation. *Remote Sensing of Environment*, *8*(2), 127—150.

Turner, D., Gower, S., Cohen, W., Gregory, M., & Maiersperger, T. (2002). Effects of spatial variability in light use efficiency on satellite-based NPP monitoring. *Remote Sensing of Environment*, *80*(3), 397—405.

Turner, D., Ritts, W., Cohen, W., Gower, S., Running, S., Zhao, M., et al. (2006). Evaluation of MODIS NPP and GPP products across multiple biomes. *Remote Sensing of Environment*, *102*(3–4), 282—292.

Turner, D., Ritts, W., Cohen, W., Maeirsperger, T., Gower, S., Kirschbaum, A., et al. (2005). Site-level evaluation of satellite-based global terrestrial gross primary production and net primary production monitoring. *Global Change Biology*, *11*(4), 666—684.

Vermote, E., Tanré, D., Deuzé, J., Herman, M., & Morcrette, J. (1997). Second simulation of the satellite signal in the solar spectrum, 6S: An overview. *IEEE Transactions on Geoscience and Remote Sensing*, *35*(3), 675—686.

Weng, J., Liao, T., Hwang, M., Chung, C., & Lin, C. (2006). Seasonal variation in photosystem II efficiency and photochemical reflectance index of evergreen trees and perennial grasses growing at low and high elevations in subtropical Taiwan. *Tree Physiology*, *26*, 1097—1104.

Wolfe, R., Roy, D., & Vermote, E. (1998). MODIS land data storage, gridding, and compositing methodology: Level 2 grid. *IEEE Transactions on Geoscience and Remote Sensing*, *36*(4), 1324—1338.

Yuan, W., Liu, S., Zhou, G., Zhou, G., Tieszen, L., Baldocchi, D., et al. (2007). Deriving a light use efficiency model from eddy covariance flux data for predicting daily gross primary production across biomes. *Agricultural and Forest Meteorology*, *143*(3–4), 189—207.